Hydrophilization of Microporous Polypropylene Celgard® Membranes by the Chemical Modification Technique

D. H. GARG,[1] W. LENK,[2] S. BERWALD,[2,*] K. LUNKWITZ,[2] F. SIMON,[2] and K.-J. EICHHORN[2]

[1]Research Center, GSFC Ltd., Fertilizernagar-391750, Baroda, India, and [2]Institute of Polymer Research Dresden, Hohe Strasse 6, 01069 Dresden, Germany

SYNOPSIS

Microporous hydrophobic polypropylene (PP) membranes (Celgard® 2400 and 2500) were modified by the chemical modification technique to impart permanent hydrophilicity. The modification was carried out in two stages. In the first stage, the membranes were hydroxylated by treatment with aqueous potassium peroxydisulfate solution under a strong flow of nitrogen. In the second stage, the hydroxylated membranes were subjected to grafting of acrylamide using cerric ammonium nitrate as an initiator. Subsequently, acrylamide grafted PP membranes were partially hydrolyzed to have carboxyl functional groups at the membrane surfaces. Under given experimental conditions the grafting also took place within the pores of the microporous structure of hydrophobic PP Celgard® membranes. Modified membranes exhibited permanently wettable characteristics by aqueous solutions and appeared translucent when immersed in water. Contact angle measurements showed excellent wetting properties with water. In contrast to unmodified Celgard® membrane, the modified membranes exhibit water permeability even after repeated drying. Membranes were further characterized by FTIR and ESCA for the different types of functional groups. © 1996 John Wiley & Sons, Inc.

INTRODUCTION

Microporous polyolefinic membranes are relatively inert, hydrophobic, and nonwettable with water. There is therefore much interest in modification of the membranes to improve hydrophilicity and to functionalize surfaces. Interest in a number of applications for hydrophilic membranes has increased, for example, biomedical,[1,2] biosensors,[3] immobilization of proteins/enzymes,[4,5] biotechnology,[6] pervaporation,[7,8] electrodialysis,[9,10] and also in a number of stringent alkaline battery applications as battery separators.[11-13] Several different methods are reported in the literature for the hydrophilization of the membranes. One of the simplest modification methods is to treat the membranes with hydrophilizing agents such as alcohols,[14] surfactants,[15,16] polyelectrolyte complexes,[17] or a coating with hydrophilic compounds.[18,19] However, it is difficult to sustain the initial hydrophilicity. The micropores of the alcohol wetted membranes sustain hydrophilicity during immersion in water; but once the membrane is dried, the hydrophilicity is instantly lost.[14] In the case of surfactant impregnated membranes, the hydrophilicity decreases with time as the surfactant tends to leak out from the pores.[20] Although these techniques are extremely simple, they do not impart permanent hydrophilicity to the membranes because the tensides or surfactants adsorb only physically and do not bind chemically to the surface of the membrane.

Further conventional methods for hydrophilization of polymeric materials, which introduce hydrophilic groups, include irradiation with UV rays,[21,22] corona discharge,[23,24] flame treatment,[25,26] oxidizing chemical treatment,[27,28] oxidizing gas treatment,[29,30] etc. When these methods are employed, an excellent hydrophilicity may be attained immediately after the treatment; but hydrophilicity deteriorates over a time, presumably because the hydrophilic groups formed on the plastic surface are rotated and buried in the in-

* To whom correspondence should be addressed.

Journal of Applied Polymer Science, Vol. 60, 2087–2104 (1996)
 CCC 0021-8995/96/122087-18

terior of the plastics due to microscopic movements of the polymer.[14,31]

Recently, more complex and advanced technologies are being used to change, modify, or improve the surface properties of membranes. Some of the key surface modification technologies are plasma treatment,[3,32] plasma polymerization,[2,33] plasma-induced graft polymerization,[5,8,34] high energy radiation (γ radiation,[35] electron beam radiation[36-38]) induced graft polymerization, etc. However, these techniques are complicated, require special equipment, and are expensive as well as time consuming. It is also known that surface modification of membranes with the plasma technique, again to provide the membrane with desirable hydrophilic properties, is effective only on the outer surface of the pores. On the other hand, the modification of pores, and particularly their inner walls, materially influences the behavior and desired properties of permanent hydrophilicity. Therefore, it is necessary to extend a kind of modification method that can modify the interior pore surface of a membrane. To obtain these results, it is necessary to modify the membrane chemically by grafting polar monomers onto the surface and also within the pore surface of the membrane.[20]

Recently, Bamford and Al-Lamee[39] reported a simple chemical modification method for the surface functionalization and grafting of polar monomers onto microporous polypropylene (PP) hollow fibers and also onto nonporous polymeric films, which provides excellent hydrophilicity to the polymeric surfaces. It is a two-stage process of which the first is hydroxylation of polymer films and the second is grafting of polar monomers onto the hydroxylated films. Hydroxylation is achieved by a reaction in an aqueous solution of potassium peroxydisulfate at 60–100°C with vigorous nitrogen purging. The grafting of polar monomers is carried out by using the conventional cerric ion technique. This technique is simple and no special equipment is needed for the modification of polymeric films. The present article deals with the functionalization of the microporous PP membranes to improve their hydrophilic properties permanently.

EXPERIMENTAL

Materials

Porous PP membranes (Celgard® 2400 and 2500) were obtained from M/S Hoechst AG (Frankfurt/Main, Germany). Their physical properties are as follows[40]:

	Celgard® 2400	Celgard® 2500
Thickness (μm)	22.9–27.9	22.9–27.9
Pore size (nm)	50 × 125	75 × 250
Percentage porosity	28–40	37–48

Cerric(IV) ammonium nitrate (PA grade) and potassium peroxydisulfate (PA grade) were purchased from Fluka and used without further purification. Acrylamide was purchased from Apolda (Germany) and used for grafting without purification. Reactive Black 5 (Remazol Black) and Trypan Blue were obtained from Aldrich and Fluka, respectively.

Hydroxylation of PP Membranes

The microporous PPs were first wetted by impregnating with methanol for 1 h, and then the methanol in the pores was replaced with distilled water before carrying out the oxidation reaction. It was expected here that the wetting of the membranes is necessary so that the oxidizing reagent can wet the membrane surface and the inner surface of the pores uniformly.

The water-primed membranes were treated with an aqueous solution of potassium peroxydisulfate with nitrogen purging for a period varying from 10 to 120 min at 80°C. Ten percent (w/v) concentration of $K_2S_2O_8$ was used for the hydroxylation of the membranes. Membranes were removed from the reaction flask, washed copiously with distilled water, and the resulting hydroxylated membranes were preserved in wet conditions until the grafting with acrylamide was carried out. Some of the hydroxylated membranes were dried in a vacuum oven at 60°C for 24 h before surface characterization.

Grafting of Hydroxylated PP Membrane

Hydroxylated membranes were subjected to grafting reaction in an aqueous solution with the cerric ion technique.[39] Cerric ammonium nitrate concentration (2×10^{-3} mol/L) in nitric acid (0.04*N*) was used in all the grafting experiments. The grafting was carried out at 50°C under a stream of nitrogen. Acrylamide in 0.1–5.0% (w/v) concentrations were taken for the grafting. The grafted membranes were removed from the reaction flask and washed with hot water to remove ungrafted homopolymer from the surfaces and the pores. Finally, grafted membranes were washed in an ultrasonic bath containing water for 15 min and allowed to dry before carrying out water permeability measurements. Some of the grafted membranes were also extracted with water

in a Soxhlet apparatus for 24 h to ensure the removal of free homopolymers from the membranes. The degree of grafting, G (%), was determined by the percentage increase in weight.

$$G = [(W_g - W_0)/W_0] \times 100$$

where W_0 and W_g represent the weights of initial and grafted membranes, respectively.

Hydrolysis of Acrylamide-Grafted PP Membranes

After the above treatment the acrylamide-grafted polypropylene membranes were partially hydrolyzed to carboxyl functional groups by heating in 1N NaOH solution for 15 min at 60°C under nitrogen atmosphere. The overall reaction scheme of the chemical modification of the PP membrane is shown in Figure 1.

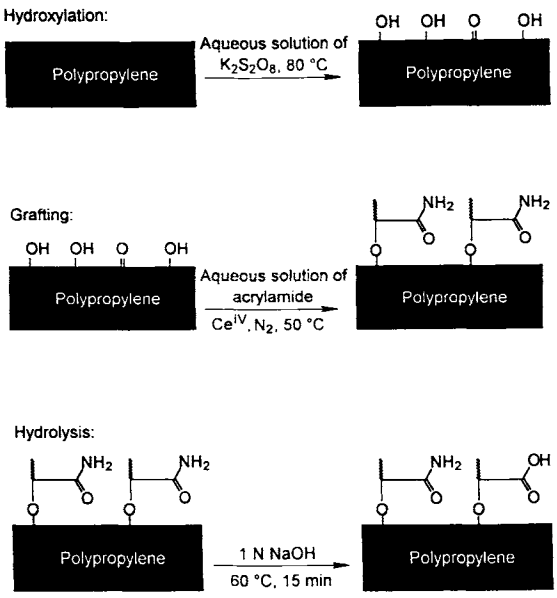

Figure 1 Schematic diagram of the chemical modification of the microporous polypropylene membrane.

Measurements

Pure Water Permeability Measurements

The grafted membranes were characterized for the pure water permeability with an Amicon-8200 test cell. The membranes with the effective area of 28.7 cm^2 were set in the test cell and the pure water permeability test was carried out by applying 4 bar pressure to the feed side. The quantity of water permeated through the membrane was measured as permeability rate or flux (Q = L/m^2 h).

Contact Angle and Wettability Test

The measurement of the contact angle between water and a membrane surface is one of the easiest ways to characterize the hydrophilicity of a membrane surface. When water is applied to the surface, the outermost surface layers interact with the water. A hydrophobic surface with low free energy gives a high contact angle with water, whereas a wet high-energy surface allows the drop to spread, i.e., gives a low contact angle.

The measurements of the contact angle of water were carried out with an instrument from M/S Krüss (No. G-40) at 25°C. The contact angles reported here were measured when the water drop moved over the dry surface, the so-called advancing contact angle.

Characterization by FTIR/Attenuated Total Reflectance (ATR) and ESCA

IR spectroscopy is one of the most commonly used techniques for polymer characterization. This method coupled with ATR plays an important role in the identification of functional groups in the surface of polymeric materials, in particular when specimens are thick, opaque, or otherwise unsuitable for transmission analysis.

We used an IFS 66-FTIR spectrometer (Bruker) with MCT detector. Two-hundred scans/spectrum were added with 4 cm^{-1} resolution and a variable Angle ATR Unit (Graseby Specac) with a germanium element (n = 4.0) was used. The element has a variable adjustment from a 30° to 60° angle of incidence.

For ESCA measurements, a FISONS ESCAlab 220i spectrometer with a MgK$\alpha_{1,2}$ ($h\nu$ = 1253.6 eV) radiation source was used to record spectra for membrane samples. The power of the source was 300 W at 20 mA. The binding energy (BE) scale of the spectra was set on the Cu ($2p_{3/2}$) peak, BE = 932.67 eV, and the Au ($4f_{7/2}$) peak, BE = 84.00 eV. Data accumulation and analysis were performed on an IBM PC by means of the VG ECLIPSE software routine. The background of the peaks were subtracted according to the Shirley method. Fitted parameters of the component peaks were the peak maximum position, the full width half maximum (FWHM), the peak area, and the Gaussian–Lorentzian ratio.

The qualitative determination of the elemental surface composition was carried out using the spectrometer transmission function and the generally accepted Wagner's atomic sensitivity factors.[41]

Table I Hyroxylation of Celgard® Membranes by $K_2S_2O_8$ Treatment

Experiment No.	$K_2S_2O_8$ Oxidation Conditions			Water Flux of Membranes[a]		Remark
	Concn (w/v %)	Temp. (°C)	Time (min)	Wet (L/m^2 h)	Dry (L/m^2 h)	
1[b]	—	—	—	—	Nil	Flux for water
					26[c]	Flux for isopropanol
					34[c]	Flux for water after wetting with isopropanol
2	10	80	30	28.80	Nil	Flux for water
					30.00	Flux for isopropanol
					76.00	Flux for water after wetting with isopropanol
3	10	80	30	30.00	Nil	Nonwettable/opaque
4	10	80	30	26.00	Nil	Nonwettable/opaque
5	10	80	10	7.56	Nil	Nonwettable/opaque
			20	12.75	Nil	Nonwettable/opaque
			30	35.40	Nil	Nonwettable/opaque
6	10	80	10	—	Nil	Nonwettable/opaque
			20	—	Nil	Nonwettable/opaque
			30	—	Nil	Nonwettable/opaque
			60	—	Nil	Nonwettable/opaque
7[b]	—	—	—	—	Nil	Flux for water
					174[c]	Flux for isopropanol
					417[c]	Flux for water after wetting with isopropanol
8	10	80	30		Nil	Nonwettable/opaque
9	10	80	30	21.53	Nil	Nonwettable/opaque
10	10	80	30	37.50	Nil	Nonwettable/opaque
11	10	80	30		Nil	Nonwettable/opaque
12	10	80	30	64.00	Nil	Nonwettable/opaque
			60	14.00	Nil	Nonwettable/opaque
			90	12.00	Nil	Nonwettable/opaque
13	10	80	30	34.30	Nil	Nonwettable/opaque
14	10	80	30	42.10	Nil	Nonwettable/opaque
15	10	80	30	38.50	Nil	Nonwettable/opaque
16	10	80	30	63.70	Nil	Nonwettable/opaque
17	10	80	30	64.00	Nil	Nonwettable/opaque

Experiments 1–6 and 7–17 are modifications of Celgard® 2400 and 2500 membranes, respectively.
[a] Water flux measured at 1 bar.
[b] Unmodified membranes, i.e., without treatment with $K_2S_2O_8$.
[c] Values obtained from the literature.[40]

During the measurements, the spectrometer was working with a constant pass energy of 25 eV.

RESULTS AND DISCUSSION

Hydroxylation of Celgard® 2400 and 2500 Membranes

Celgard® PP membranes were functionalized by carrying out oxidation in the presence of a 10% aqueous solution of potassium peroxydisulfate at 80°C under a continuous flow of nitrogen. The experimental conditions and results are shown in Table I for Celgard® 2400 and 2500. The direct evidence of introduction of hydroxyl groups into the membrane matrix was observed by coupling with the reactive dye Remazol Black, which gave a permanent blue tint; unmodified membrane gave a negative result. The reaction mechanism for the functionalization of PP membrane is shown in Figure 2 as reported by Bamford and Al-Lamee.[42] Schemes I and

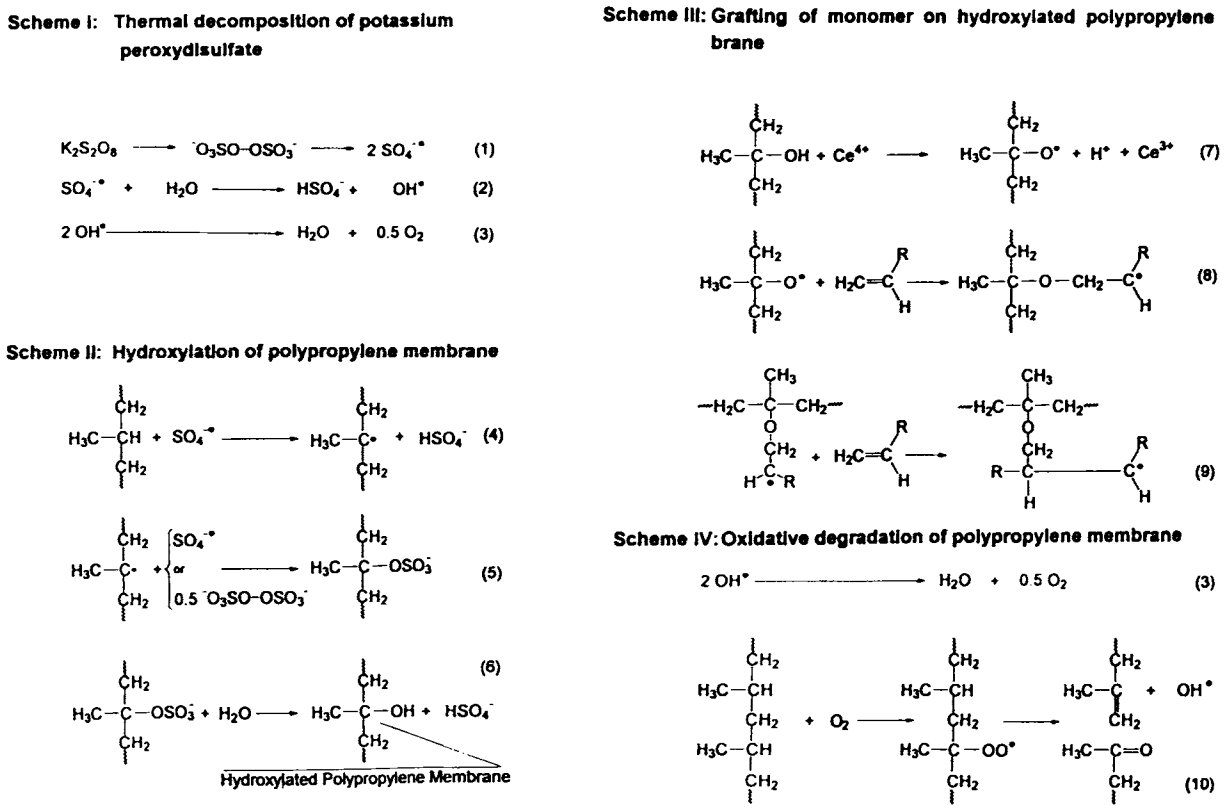

Figure 2 Reaction mechanism for various steps during the functionalization of microporous polypropylene membranes.[42]

II of Figure 2 show the reaction mechanism for hydroxylation of the PP membrane.

Effect of Oxidation Time

The PP membranes were treated with oxidizing reagent for different periods of time. The membranes were found to be damaged when treated for prolonged periods i.e., for more than 2 h, which is mainly due to oxidative degradation. A generally accepted reaction mechanism is that a polymer radical reacts with an oxygen molecule to form a peroxy radical.[43] The peroxy group can undergo various chemical reactions yielding keto, aldehyde, and unsaturated functional groups as shown in Figure 2 (Scheme IV). However, the degradation of PP membranes was not observed when treated for less than 2 h.

Supposedly oxidative degradation leads to the formation of hydroperoxide groups onto the PP backbone when irradiated with high energy radiations or treated with plasma in the presence of air.[44,45] But we could not detect peroxide groups on the surface of the membranes, either by the potassium iodide test or by carrying out redox polymerization of acrylamide in the presence of aqueous ferrous sulfate solution. The presence of peroxide groups on the surface would have initiated the polymerization of acrylamide in the presence of ferrous sulfate.[46,47] The results of the redox polymerization were negative, indicating the absence of peroxide groups on the surface of hydroxylated PP membranes. Hydroxylated membranes were further characterized with ATR for the detection of hydroperoxide groups. As described in the literature,[44] the absorption band of the hydroperoxide group appears at 3350 cm^{-1}. However, our FTIR analysis on both transmission and internal reflection modes for the hydroxylated membrane does not show any absorption peak at 3350 cm^{-1}. The emission peak for hydroperoxide groups appears in the range of 535.1–536 eV in the O(1*s*) spectrum of ESCA.[48] However, the ESCA scans taken for the hydroxylated PP do not reveal any emission peak in the O(1*s*) spectrum at 535.2 eV corresponding to hydroperoxide groups.

Characterization of Hydroxylated Membranes

Measurements of Water Permeability

The measurements of pure water permeability were carried out for the hydroxylated membranes with

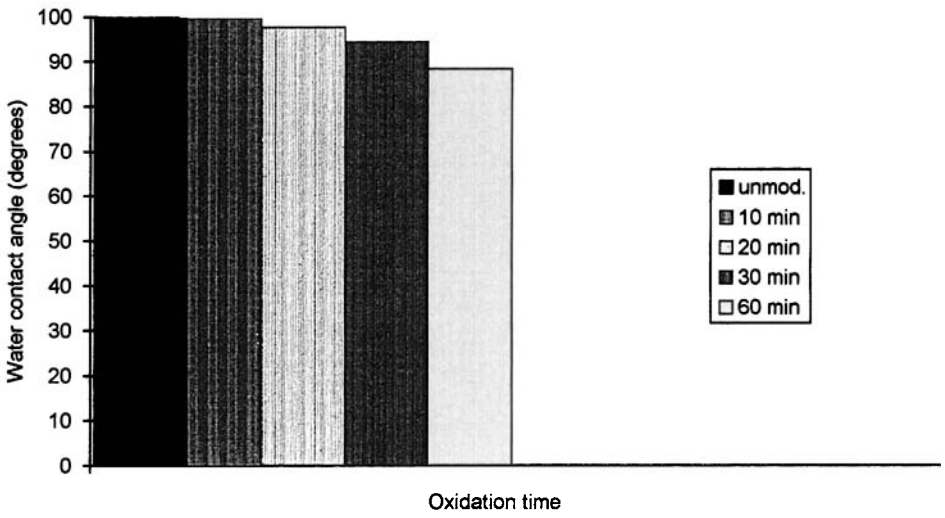

Figure 3 Water contact angle measured for hydroxylated membranes at different oxidation periods.

the use of a Millipore test cell. The water flux was observed for the hydroxylated membranes when measured immediately after the hydroxylation reaction for the wet membranes. However, water flux could not be observed when it was measured again after drying of the same membranes.

The wet membranes show the flux of water after the hydroxylation step because they were already primed with alcohol and finally with water to be wetted with the oxidizing reagent before carrying out the reaction. The membranes lost their wettability with water when dried. The variation in the water flux was observed when measured in the wet condition, after the hydroxylation step, due to the difference in wetting properties after the reaction. So, it was difficult to correlate with the experimental conditions.

It was expected here that the hydroxylation step introduces highly polar hydroxyl groups onto the membrane surface. Hence, the resulting membrane must be hydrophilic in nature and should also show water permeability after drying the membranes. In contrast to our expectation, the hydroxylated membranes did not show any water permeability. The unmodified membranes did not allow flux because they are hydrophobic in nature (Expt. 1, Table I). However, the water flux for the hydroxylated membrane could be initiated similar to unmodified membranes after wetting the membranes with alcohol and then replacing the same with water. This water flux was observed to be higher than the unmodified membrane as mentioned in Table I (Expt. 2). This could be explained on the basis that formation of larger pores takes place due to the damage of the fibril structure between the pores by the oxidizing reagent.

Water Contact Angle Measurements

The wettability of the hydroxylated membranes was characterized by water contact angle measurements. The values obtained for the hydroxylated membranes are graphically represented in Figure 3. The water contact angle measurements were carried out immediately after the drying of membranes after the hydroxylation reaction.

Water contact angles measured for hydroxylated membranes were found to be similar to those of unmodified PP membranes as seen in Figure 3. Only a marginal tendency to decrease the contact angle with increasing oxidation time was observed. It was expected that the water contact angle for the hydroxylated membranes would be smaller, due to higher surface energy by introduction of highly polar hydroxyl groups onto the membrane surface. However, the observed larger contact angle indicates that the membrane surface is hydrophobic in nature and the hydroxyl groups formed during the oxidation reaction may be disappearing from the contact angle surface on drying. This is due to the hydrophilic groups generated at the PP surface, moving and diffusing into the bulk polymer to minimize the surface energy. Surface reconstruction in which the high energy, more hydrophilic surface produced in the oxidative functionalization reactions reorganize to produce a lower energy, more hydrophobic surface

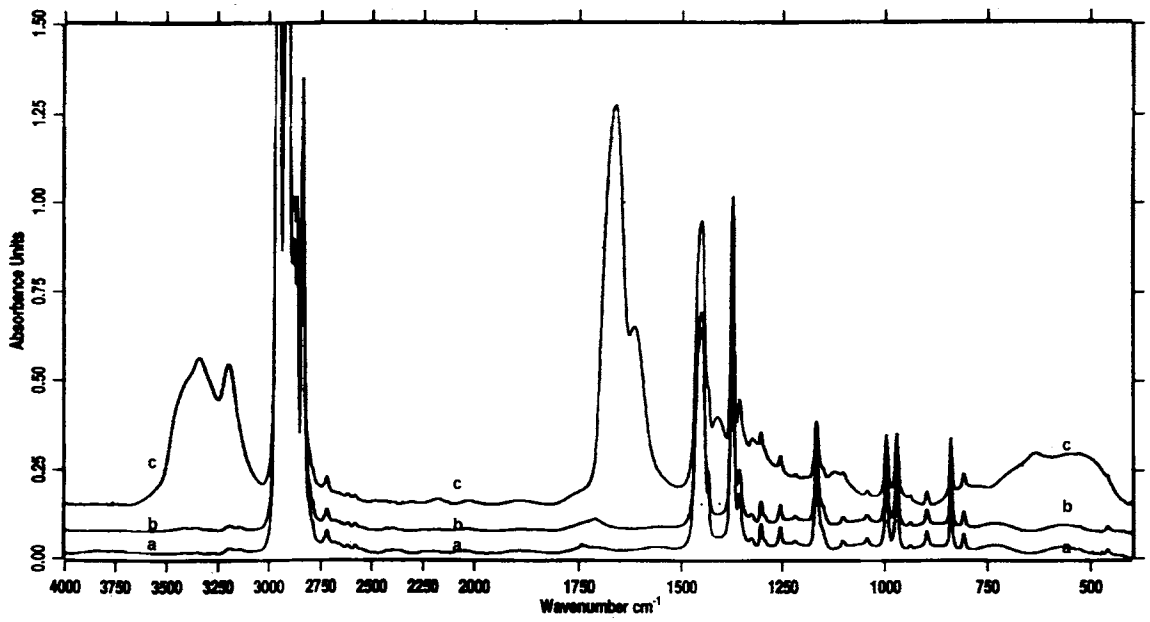

Figure 4 FTIR spectra (transmission mode) of (a) unmodified polypropylene membrane, Celgard® 2500; (b) hydroxylated polypropylene membrane (after $K_2S_2O_8$ treatment); and (c) acrylamide-grafted polypropylene membrane.

is a general phenomena for surface functionalized polymers.[49] When membranes were dried and exposed to air, hydrophobic groups and molecules tended to orientate or move toward the surface to reduce the interfacial energy. Thus, hydrophilic groups, especially polar hydroxyl groups, get buried into the bulk of the polymer, and hence a lower number of hydrophilic groups are located on the surface. Reorientation of functional groups by configurational movements of the polymer segments has been frequently reported in the literature.[50–52] Similar results have been mentioned when polyolefinic films were investigated for the surface properties after carrying out treatments such as flame treatment,[31] plasma treatment,[53,54] or plasma polymerization of polar monomers,[49] or chemical oxidative treatment with chromic acid[31] or sulfuric acid.[52] Hence, the hydroxylated membranes exhibit hydrophobic properties and they are not wettable with water and appear opaque. If hydroxyl groups are buried into the bulk of polymer but are near the surface, they should be easily detected with ATR analysis because it is a method to identify functional groups up to the depth of about 300 nm (60° Ge element) at 1800 cm^{-1} according to the Harrick equation.[55]

FTIR Analysis

The hydroxylated membranes were analyzed in the transmission mode and with ATR to identify hydroxyl groups on the surface and in the depth of the polymer, respectively. Figure 4 shows the IR transmission spectra taken for unmodified and hydroxylated PP Celgard® 2500 membranes. The spectra of unmodified [Fig. 4(a)] and hydroxylated membrane [Fig. 4(b)] are identical and no additional absorption band for hydroxyl groups can be detected in the spectrum of hydroxylated membranes. This could possibly be due to the very small concentration of OH groups compared with the bulk PP matrix measured in the transmission mode. Therefore, ATR spectra were recorded and compared for unmodified and hydroxylated membrane surfaces. ATR spectra of unmodified and hydroxylated membrane show that only small absorption PP bands corresponding to $-CH_2-$ bending and $-CH_2-$ stretching of PP occurred at 1460–1470 and 2900–3000 cm^{-1}, respectively.[3] However, no additional absorption band could be detected from the spectrum of the hydroxylated membrane. Both spectra were identical, again indicating the disappearance of hydroxyl groups from the surface on drying. Note that it is difficult to obtain good ATR spectra of porous membranes because the necessary contact between the rough membrane surface and the Ge crystal could not be realized. It should be considered that a migration of OH groups from the hydroxylated surface into the depth of the polymer matrix were sometimes discussed. Therefore IR analysis does not reveal any information about the presence of hydroxyl groups

on the surface or in the hydroxylated membrane. In view of this the membrane surface was analyzed with ESCA.

ESCA Analysis

In an attempt to gain further information about the composition of the surface of the hydroxylated membranes, membranes were subjected to ESCA. Figure 5 shows the ESCA survey scan for the unmodified and modified Celgard® 2500 PP membranes at different stages of surface modification.

As shown in Figure 5(a) for unmodified PP membrane, a major emission peak corresponding to 285-eV binding energy of C(1*s*) was detected and a minor emission peak corresponding to oxygen was observed that might be caused by the impurities or additives initially present in the polymer. A similar emission peak was also reported by Wang et al.[3] for the PP Celgard® 2500 membranes. The ESCA survey scan for the hydroxylated membrane shows the three peaks corresponding to C(1*s*), N(1*s*), and O(1*s*), respectively. An additional emission peak of nitrogen could be explained on the basis that the oxidation of the membrane was carried out under vigorous flow of nitrogen, and hence it could be incorporated as primary amine or amide groups onto the surface. Recently, Poncin–Epaillard et al.[44] reported nitrogen emission peaks in the ESCA spectrum of electron beam irradiated PP film. They discussed the formation of primary amine when the PP films were treated with electron beam irradiation in the presence of air.

The high resolution spectra of hydroxylated Celgard® 2500 PP membrane corresponding to C(1*s*), O(1*s*), and N(1*s*) are shown in Figure 6 in order to see different types of functionalities at the membrane surface. Table II summarizes the results of the functional groups determined by ESCA.

The C(1*s*) spectrum of hydroxylated membrane deconvoluted into four peaks is shown in Figure 6(a). Peak D corresponds to C—H and C—C at a binding energy of 285.00 eV. The peak maximum for peak C (286.20 eV) may be considered to be the alcohol groups (C—OH) or in the expected range of binding energy of C—O—C groups that may be due to inter- or intramolecular interactions between C—OH groups at the membrane surface yielding in the formation of a hydrogen bridge. Peak B (287.64 eV) corresponds to the binding energy of the carbonyl group that could be mainly expected as a ketone group because primary aldehyde groups are generally very reactive and may possibly undergo chemical reactions to build up either primary amine or amide groups under experimental conditions.

Peak A (288.53 eV) can be considered for the presence of amide functional groups. The high resolution C(1*s*) spectra of acrylamide grafted PP membrane [Fig. 6(a)] shows the presence of amide functional groups at the binding energy 288.17 eV that has a shift of only 0.36 eV at lower emission energy in comparison to the emission energy of peak A of the hydroxylated membrane. Therefore, peak A can be considered for the presence of amide functional groups. The formation of amide functional groups onto the surface of hydroxylated membrane can be possibly due to the reaction between aldehyde or ketone groups formed during the oxidation reaction and reactive nitrogen as shown in the following:

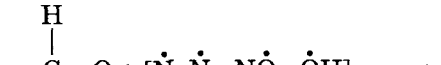

Aldehyde

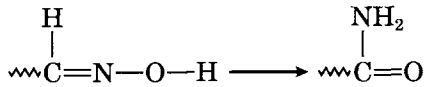

Oxime **Amide**

Figure 6(b) shows the high resolution spectra of O(1*s*) for the hydroxylated PP membrane that has been resolved into three peaks. Peak C (531.46 eV) is possibly due to the amide group, because the binding energy for the oxygen of the amide functional group is mentioned in the range of 531.30–532.0 eV.

Peak B can be interpreted for the oxygen of the carbonyl groups and also for the alcohol oxygen. However, the peak ratio for [C]/[B] = 0.6954 does not correspond to the peak ratio in the C(1*s*) spectrum ([A]/[B] + [C] = 0.1330). Besides this, it is also necessary to explain the presence or shifting of peak A in the O(1*s*) spectrum.

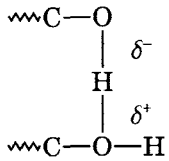

Hydrogen bridge

Higher density of hydroxyl groups on the surface of the hydroxylated membrane lead to the formation of a hydrogen bridge. This results in the building of higher electron density on the electron receiving C—OH groups, whereas the electron donating groups have a partially positive charge. A partial

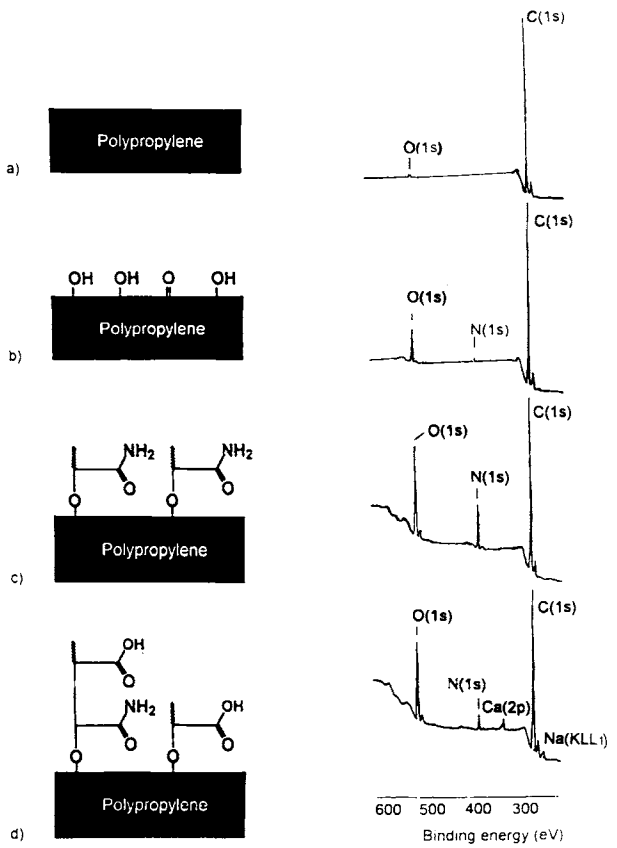

Figure 5 ESCA survey scan for the unmodified and modified polypropylene membranes, Celgard® 2500, at different stages of modification.

positive charge shifts the oxygen peak to higher binding energy, which indicates the strong shifting of peak A. Similarly the emission peak for the oxygen having higher electron density shifts to the lower binding energy and contributes partly to peak C, which yields higher value for peak C of O(1*s*). If the ratio of {[C] − [A]/[A] + [B] + [C] = 0.1717} is considered, where [C] − [A] corresponds to amide group concentration in the O(1*s*) spectrum, and the ratio for the amide groups corresponding in the C(1*s*) spectrum {[A]/[A] + [B] + [C] = 0.117} is compared, then the obtained values are almost correlative. Hence, the emission peak A in the O(1*s*) spectrum corresponds to the carbonyl groups. Figure 6(c) shows the N(1*s*) high resolution spectrum having mainly one peak with a small apex shifted to higher energy. The binding energies corresponding to these peaks do not give any clear indication about the type of nitrogen group. Amine groups are generally reported in the range of BE = 399–400 eV,[56]; amide groups are in the range of BE = 399.7–400 eV,[56] which corresponds to the peak maximum of peak B (399.6 eV).

Peak A could be considered for the protonated form of the amide groups. The values given are for the protonated amide or amine groups in the range of 401.46–402.14 eV.[56] It is worth mentioning that protonated and deprotonated functional groups are always found in equilibrium due to inter- and intramolecular acid–base interactions. The characterization of hydroxylated membranes with ESCA supplied the information about the presence of hydroxyl groups on the surface. However, FTIR analysis, water contact angle measurements, and water permeability study suggest that the hydroxyl groups disappear from the surface and get buried in the depth of the polymer when the membrane is dried. The environment around the membrane surface plays a very important role for the surface functionalized polymers by maintaining their hydrophilic properties at the surface. In view of this the hydroxylated membranes were preserved in wet conditions under water until the grafting with acrylamide was carried out.

Acrylamide Grafting onto PP Surface

The hydroxylation step is essential for the grafting of acrylamide onto the surface and the membranes should be preserved in a wet condition. To prove this, the hydroxylated Celgard® 2500 membranes were grafted with acrylamide immediately after the treatment, after preserving in a wet condition and drying the membrane, and also with nonhydroxylated membrane. The results are shown in Table III.

It was found that a higher percentage of grafting was obtained when membranes were subjected to the acrylamide grafting immediately after the hydroxylation step without drying the membrane. The grafting efficiency was found to decrease when preserved for 24 h in a wet condition and almost negligible grafting was observed when membranes were used after drying. The nonhydroxylated membrane did not show any grafting onto the surface. The membranes grafted with a higher percentage of acrylamide had excellent wettability and appeared translucent when immersed in water.

The membrane also appears translucent when grafting of the polar monomer takes place within the porous structure of the membrane.[2] After drying in a vacuum the acrylamide-grafted membrane appeared opaque upon immersing in water, indicating that the grafting had taken place only on the surface of the membrane; however, the nonhydroxylated membrane appeared opaque and did not wet with water. In view of this, the hydroxylated membranes

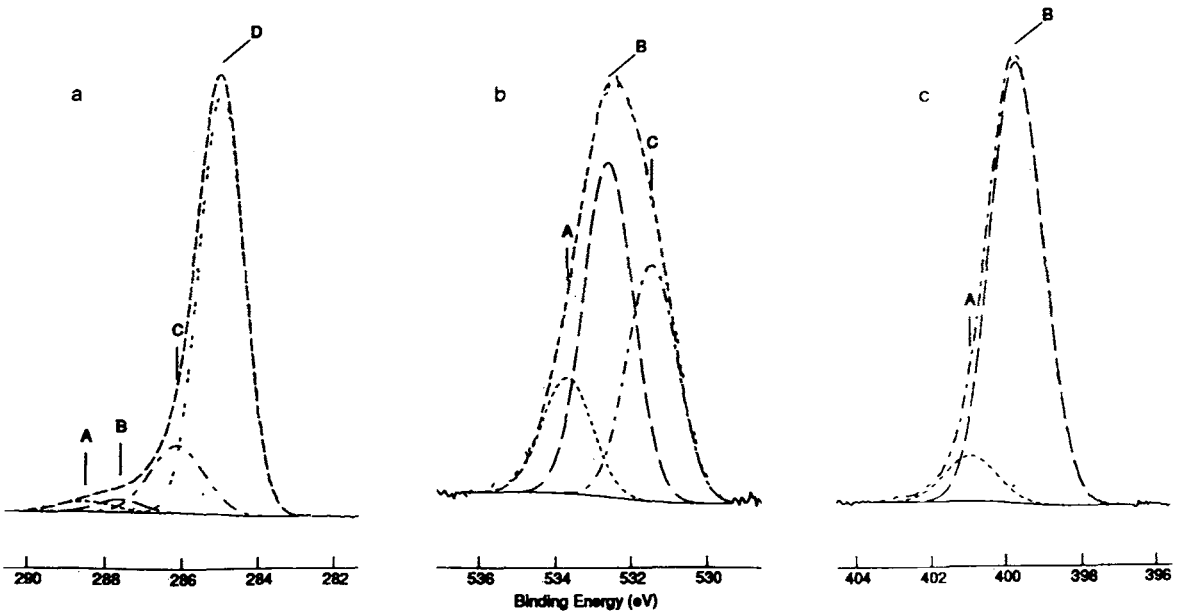

Figure 6 High resolution ESCA spectra (satellites substracted) for the hydroxylated polypropylene membrane, Celgard® 2500: (a) C(1*s*) spectrum, (b) O(1*s*) spectrum, and (c) N(1*s*) spectrum.

were subjected to grafting immediately after the oxidation treatment.

The conditions for the acrylamide grafting and test results are shown in Table IV for the Celgard® 2400 and 2500 membranes. The acrylamide-grafted membranes with higher concentrations of acrylamide, i.e., 2.5 and 5% (w/v) were wettable with water and translucent when immersed in water even after drying. The grafted membranes also exhibited a pure water flux that is almost the same when measured both before and after drying. This shows that the acrylamide-grafted membranes do not need to be primed with the wetting agent to initiate the water flow. However, the water flux was considerably low. This could be explained on the basis that the grafting of acrylamide plugs the pores of the membrane and hence reduces the effective free cross section for the water flow. Polyacrylamide grafted into the pores will also swell within the pores and subsequently reduce the free flow of the water expected, by reducing the effective area of the porous volume of the membrane.

Acrylamide Grafting onto Celgard® 2400 Membranes

Celgard® 2400 membranes were treated with the 10% (w/v) aqueous solution of potassium peroxydisulfate for a different period of time as shown in Table IV. The resulting hydroxylated membranes were subjected to acrylamide grafting with different concentrations of acrylamide, 5 and 2.5% (w/v), as shown in experiments 5 and 6, respectively.

The pure water flux observed for the acrylamide-grafted membranes after 10 min of hydroxylation treatment was higher in both cases and it was found to decrease with the increase in the hydroxylation treatment time. A higher hydroxylation time introduces a higher concentration of hydroxyl groups on the membrane surface and also the inner surface of the pores that subsequently results in a higher percentage of acrylamide grafting, which yields a lower water flux. The acrylamide-grafted membranes with a lower 2.5% (w/v) concentration of acrylamide show a higher flux than the membranes grafted with the 5% (w/v) concentration of acrylamide. This could again be explained on the basis of the lower polymer density on the membrane surface when modified with lower concentration. The acrylamide-grafted membranes were water wettable and translucent when immersed in water. When nonhydroxylated membranes (i.e., without treatment with potassium peroxydisulfate) were subjected to acrylamide grafting, they did not show any grafting of acrylamide onto the membranes (experiments 5a and 6a) and were found nonwettable with water, looked opaque when immersed in water, and allowed no flow of pure water.

Table II ESCA Data of Unmodified and Modified Celgard Membranes

Sample	Peak	Position (eV)	2σ = FWHM (eV)	Assignment	Intensity (%)
Unmodified membrane	C(1s)	285.00	1.27	C_xH_y traces of C—O components	≈ 99
		> 285			≈ 1
	O(1s)	532.96	1.67	C—O	39.60
		531.64	1.67	C=O and inorg. impurities	60.40
	N(1s)			Has not been detected	
Hydroxylated membrane	C(1s)	288.53	1.67	C(O)—NH_2	2.41
		287.64	1.36	C=O	2.41
		286.20	1.67	C—OH	15.63
		285.00	1.36	C_xH_y	79.51
	O(1s)	533.71	1.55	C—O	16.92
		532.61	1.55	C=O	49.00
		531.46	1.55	C(O)NH_2	34.08
	N(1s)	401.73	1.84	C(O)N^+H	4.90
		399.96	1.84	C(O)NH	95.10
Amide-grafted membrane	C(1s)	288.17	1.63	C(O)—NH_2	22.98
		287.54	1.63	C=O	1.53
		286.21	1.63	C—OH	7.55
		285.00	1.60	C_xH_y	67.94
	O(1s)	533.88	1.70	C—O	3.42
		532.73	1.70	C=O, C(O)N^+H	1.82
		531.45	1.70	C(O)NH_2	81.76
	N(1s)	400.95	1.65	C(O)N^+H	9.28
		399.70	1.65	C(O)NH	90.72
Partially hydrolyzed membrane	C(1s)	289.27	1.63	C(O)—O	2.29
		288.25	1.63	C(O)—NH_2	15.64
		287.43	1.63	C=O	1.37
		286.32	1.63	C—OH	11.22
		285.00	1.63	C_xH_y	69.46
	O(1s)	533.65	1.68	C—O	17.53
		532.34	1.68	C=O, C(O)N^+H	56.50
		531.35	1.68	C(O)NH	25.97
	N(1s)	400.56	1.68	C(O)N^+H	32.27
		399.70	1.68	C(O)NH	67.73

Acrylamide Grafting onto Celgard® 2500 Membranes

Celgard® 2500 membranes were modified similarly to the Celgard® 2400 membranes and the results are shown in Table IV. In this case the acrylamide concentration was varied from 5 to 0.1% (w/v). The grafted membranes were extremely hydrophilic when grafted with higher than 2.5% (w/v) concentration of acrylamide. The membranes were water wettable and translucent when immersed in water. These membranes exhibited pure water flux when measured immediately after the reaction in wet conditions and also after drying. However, the water flux was very low. To improve the flux of the membranes, it was decided to reduce the concentration of acrylamide during grafting, so that there would be a lower percentage of grafting onto the membrane surface.

When the acrylamide concentration was reduced from 2.5 to 0.1% (w/v), the resulting membranes were found to be opaque and did not exhibit any water flux after drying. However, these membranes allowed water flux when measured in wet conditions because they were already prewetted before carrying out the grafting. This wetting property was lost when

Table III Grafting of Acrylamide onto Hydroxylated Celgard® 2500 Membranes Preserved in Different Conditions

Surface Conditions	Grafting (%)	Water Flux of Membranes		Wettability after Drying
		Wet (L/m^2 h)	Dry (L/m^2 h)	
I. Immediately after hydroxylation step	78.04	2.23	2.30	Excellent/translucent
II. After preserving in wet condition by immersing in water for 24 h	31.70	2.75	2.80	Excellent/translucent
III. After drying in vacuum for 24 h at 25°C	7.30	Nil	Nil	Partial/opaque
IV. Inmodified membrane (without hydroxylation step)	No grafting	Nil	Nil	None/opaque

Experimental conditions: acrylamide concentration 5% (w/v), [L] = 2×10^{-3} mol/L in 0.04*N* HNO_3, temperature 50°C, time 4 h.

the membranes were dried. The grafting efficiency onto the membrane surface was also found to be lower when the concentration used was lower than 2.5% (w/v). The grafted membranes appeared opaque, which indicates that no grafting had taken place in the inner surface of the pores.

The pure water flux observed for the acrylamide-grafted Celgard® 2500 membrane was found lower than Celgard® 2400. It was expected here that the modified Celgard® 2500 membrane would show a higher flux of water due to larger pore size and higher percentage porosity. However, this lower flux of water could be due to higher grafting onto the membrane surface and also within the surface of the pores. The larger pores of the Celgard® 2500 membrane have easier access to the reaction gradients that results in a higher concentration of hydroxyl groups during the oxidation treatment and hence a greater possibility of acrylamide grafting within the pore in comparison to Celgard® 2400 membranes. Hirotsu and Arita[34] also reported higher grafting on Celgard® 2500 membrane than on Celgard® 2400 membrane for the plasma modified Celgard membranes. Discrepancies in the data could be attributable to the heterogenous properties of PP membrane and also to the heterogenous nature of the acrylamide grafting, depending upon the availability of hydroxyl groups on the surface of the membrane.

Characterization of Acrylamide-Grafted Celgard® 2500 Membranes

The acrylamide-grafted membranes were analyzed for their hydrophilic properties by carrying out water contact angle measurements. The acrylamide-grafted membranes showed considerable decrease in contact angle from 99.8° to 51.3° for unmodified membranes and modified membranes, respectively, as shown graphically in Figure 7 which indicates the increase in hydrophilicity after grafting of acrylamide.

The grafting of acrylamide was confirmed by FTIR analysis as illustrated in Figure 3(c) that shows strong absorption bands at 3351, 3199, and 1664 cm^{-1} for the amide functional groups. When acrylamide grafting is carried out without treatment with potassium peroxysulfate, the membranes do not show any grafting of acrylamide. The FTIR spectrum taken for the acrylamide-grafted membrane without the hydroxylation step is shown in Figure 8. As expected, the absorption band for the amide group of acrylamide at 1664 cm^{-1} could not be detected. This indicates that the hydroxylation step is essential for the grafting of acrylamide.

ESCA Characterization

Figure 5(c) illustrates the ESCA survey scan for the acrylamide-grafted PP membrane. The atomic ratio obtained from the survey scan spectrum for [O] : [C] and [N] : [C] are 0.2510 and 0.2317, respectively, which indicates almost the same concentration of [O] and [N] with respect to carbon. This gives an idea about the surface composition of the acrylamide-grafted membrane.

Figure 9 shows the high resolution spectra of C(1*s*), O(1*s*), and N(1*s*). The C(1*s*) spectrum [Fig. 9(a)] deconvoluted in four peaks where peak D, appearing at the binding energy of 285.00 eV, corresponds to C—H and C—C. The peak maximum for peak A (288.17 eV) can be interpreted as an amide group.

The peak ratio for the amide groups {[A]/[A] + [B] + [C] + [D] = 0.2298} in the C(1*s*) spectrum is almost the same obtained for the peak ratio for nitrogen to carbon, [N] : [C] = 0.2317, in the survey

Table IV Grafting of Acrylamide onto Hydroxylated Membranes

Experiment No.	Ammonium Grafting Conditions[a] Concn (w/v %)	Temp. (°C)	Time (min)	Grafting (%)	Water Flux of Membranes[b] Wet (L/m^2 h)	Dry (L/m^2 h)	Wettability after Drying
3	5.0	50	4	32.0	6.16	5.92	Excellent/translucent
4	5.0	50	4	39.9	3.84	3.76	Excellent/translucent
5	5.0	50	4	21.6	5.84	6.12	Excellent/translucent
				27.5	3.84	4.00	Excellent/translucent
				27.6	3.96	3.84	Excellent/translucent
5a[c]	5.0	50	4	0.0	—	Nil	None/opaque
6	2.5	50	4	14.4	9.56	9.72	Excellent/translucent
				14.2	6.28	6.68	Excellent/translucent
				17.9	4.80	5.40	Excellent/translucent
				14.7	2.92	3.56	Excellent/translucent
6a[c]	2.5	50	4	0.0	—	Nil	None/opaque
8	5.0	50	4	68.4	2.76	2.88	Excellent/translucent
9	5.0	50	4	78.3	2.20	2.64	Excellent/translucent
10	5.0	50	4	65.3	2.40	2.44	Excellent/translucent
10a	5.0	50	4	0.0	—	Nil	None/opaque
11	2.5	50	4	24.6	10.40	4.92	Excellent/translucent
12	2.5	50	4	21.9	11.20	4.72	Excellent/translucent
				36.1	12.80	2.48	Excellent/translucent
				17.8	8.40	1.48	Excellent/translucent
13	2.0	50	4	8.1	21.20	Nil	Partial/opaque
14	1.0	50	4	7.3	5.60	Nil	Partial/opaque
15	0.5	50	4	8.5	7.30	Nil	Partial/opaque
16	0.25	50	4	3.2	50.00	Nil	Partial/opaque
17	0.1	50	4	1.6	65.00	Nil	Partial/opaque

Experiments 3–6a and 8–17 are modifications of Celgard® 2400 and 2500 membranes, respectively.
[a] Cerric ammonium nitrate concentration 2×10^{-3} mol/L in 0.04*N* NHO_3.
[b] Measured at 4 bar.
[c] Nonhydroxylated membrane, i.e., without $K_2S_2O_8$ treatment.

scan. The peak position corresponding to the amide groups (288.17 eV) in the C(1*s*) spectrum of acrylamide-grafted membrane, on the basis of grafting of acrylamide, indicates that the peak position appearing at the binding energy 288.53 eV in the C(1*s*) spectrum for hydroxylated membrane is due to amide groups. This confirms the formation of amide functional groups on the PP membrane surface when treated with the aqueous solution of potassium peroxydisulfate and under a vigorous flow of nitrogen. Peak B (287.54 eV for C=O) and peak C (286.21 eV for C—OH) appear at the same position as in the C(1*s*) spectrum of hydroxylated membranes and can be interpreted similarly.

Figure 9(b) shows the high resolution O(1*s*) spectrum deconvoluted into three peaks. Peak C (531.45 eV) corresponds to amide groups whereas peak B (532.72 eV) and peak A (533.88 eV) can be interpreted for C=O and C—OH functional groups, respectively.

The N(1*s*) spectrum [Fig. 9(c)] for acrylamide-grafted membrane is again resolved into two peaks similar to that of the N(1*s*) spectrum for the hydroxylated membrane. Peak B appears at almost the same binding energy of 399.70 eV, which corresponds to amide functional groups. However, shifting of peak A for the binding energy of 400.95 eV could only be explained on the basis of changes in equilibrium of protonated and deprotonated nitrogen due to a relatively lower concentration of hydroxyl groups on the surface of the membrane.

Partial Hydrolysis of Acrylamide-Grafted Membranes

Some of the acrylamide-grafted Celgard® 2500 membranes were subjected to partial hydrolysis with 1*N* NaOH solution at 60°C for a period of 15 min. After carrying out the hydrolysis the membranes

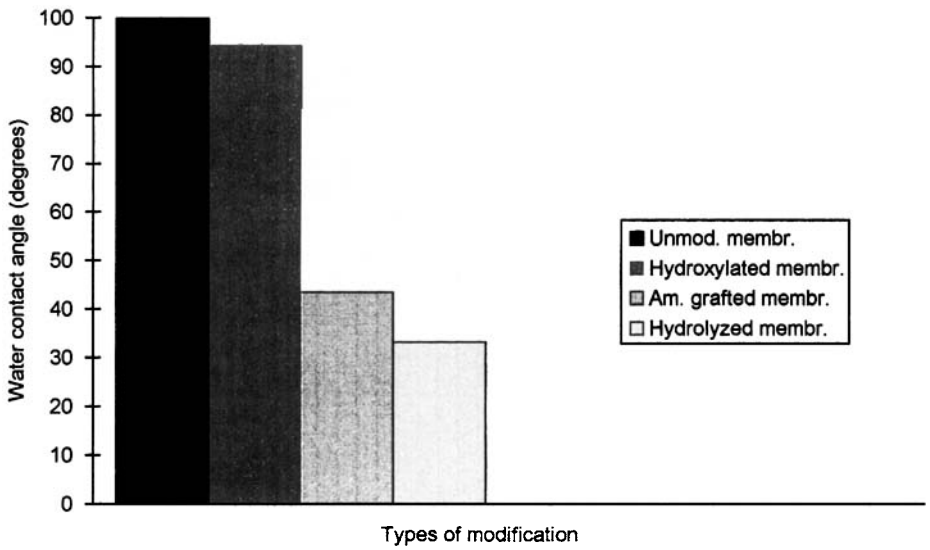

Figure 7 Water contact angle measured for different modified membranes.

were copiously washed with water and measured for pure water permeability in wet conditions and after drying. The results are shown in Table V.

The hydrolyzed membranes with a higher concentration than the acrylamide-grafted membranes, above 2.5% (w/v), exhibited water flux; the membranes grafted with a lower concentration of acrylamide did not show any water permeability when measured after drying. The partially hydrolyzed membranes were water wettable and translucent when immersed in water, but the membranes with a lower concentration were nonwettable and remained opaque. The partially hydrolyzed membranes exhibited higher water flux than the acrylamide-grafted membranes. The 33.3° water contact angle measured for the hydrolyzed membranes was also found to be smaller than the 51.3° found for the acrylamide-grafted membrane as shown in Figure 7. This indicated that the partially hydrolyzed acrylamide-grafted membranes are more hydrophilic

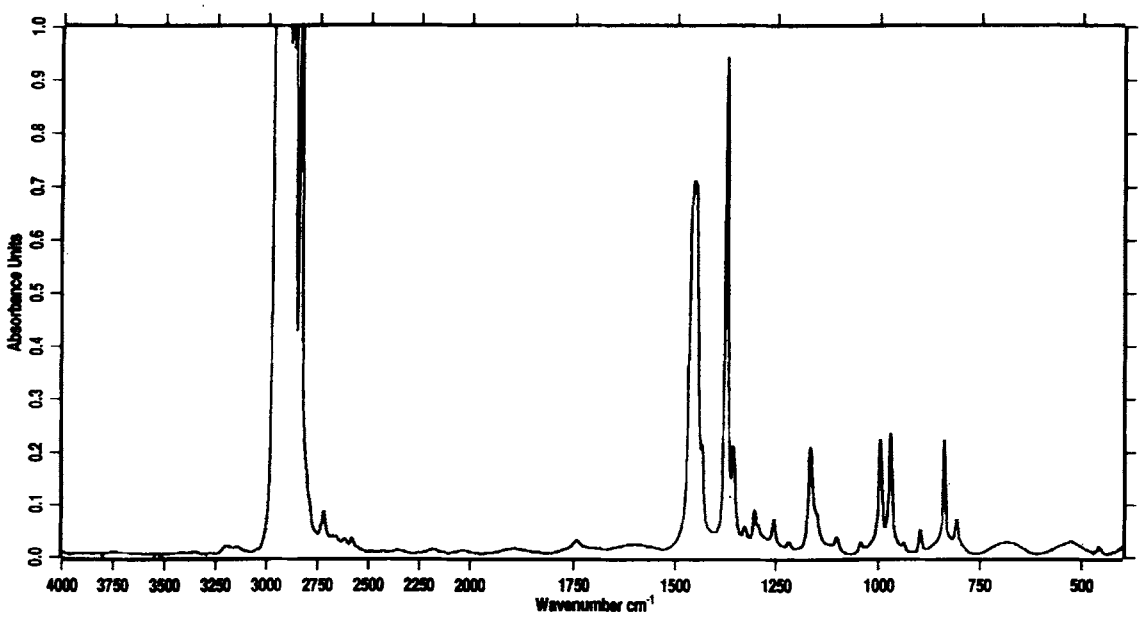

Figure 8 FTIR spectrum (transmission mode) of acrylamide-grafted polypropylene membrane, Celgard® 2500 (without $K_2S_2O_8$ treatment).

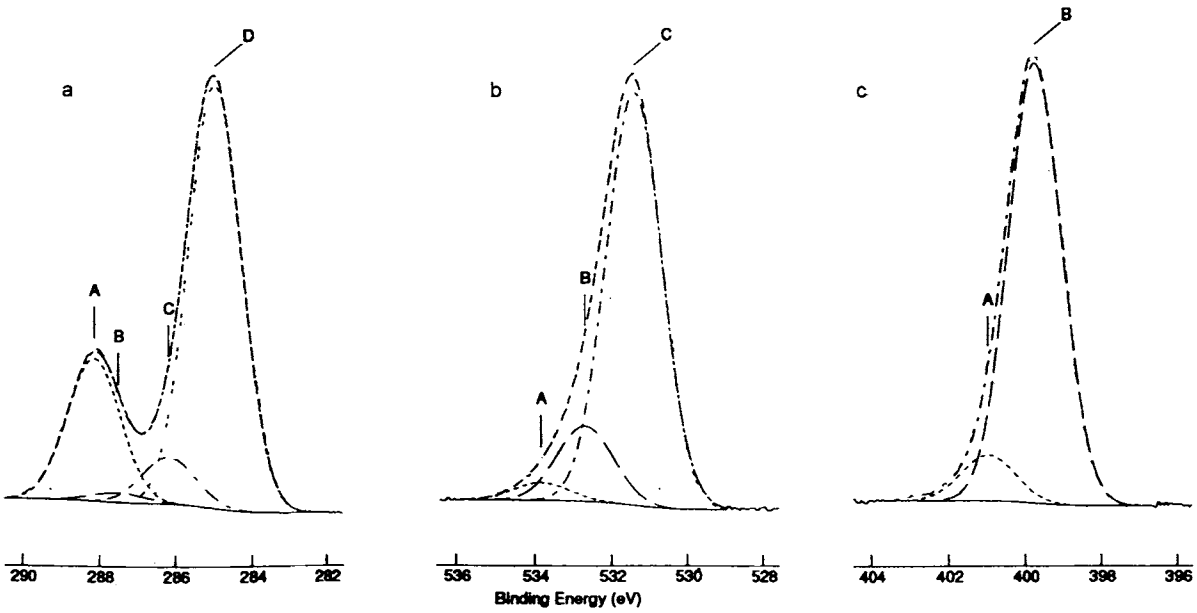

Figure 9 High resolution ESCA spectra (satellites substracted) for acrylamide-grafted polypropylene membrane, Celgard® 2500: (a) C(1*s*) spectrum, (b) O(1*s*) spectrum, and (c) N(1*s*) spectrum.

in nature. The FTIR spectrum taken for the partially hydrolyzed membrane is shown in Figure 10. The appearance of the carboxylate band at 1559 cm^{-1} corresponds with the deprotonated carboxyl groups.[8] The presence of an absorption band at 1664 cm^{-1}, corresponding to the amide functional groups, beside the carboxylate band indicates the partial hydrolysis of polyamide segments.

Figure 5(d) shows the ESCA survey scan for the hydrolyzed PP membranes, whereas Figure 11 shows the high resolution spectra of C(1*s*), O(1*s*), and N(1*s*). The C(1*s*) spectrum is shown in Figure 11(a) deconvoluted into five peaks. Peak A (289.27 eV) corresponds to carboxyl groups on the surface, which also confirms the partial hydrolysis of amide groups into carboxyl groups. Peak B (288.25 eV) corresponds to the remaining amide functional groups.

Peak C shows the presence of carbonyl groups of ketones. Peak D (286.32 eV) contains the component peak for alcohol groups and the β shift of the carboxyl groups, and the main peak E appears at 285.00 eV for C_xH_y.

The O(1*s*) spectrum [Fig. 11(b)] resolves into three peaks like the O(1*s*) spectrum of the acrylamide-grafted PP membrane. However, the intensities of the component peaks have been changed. Through the carboxyl groups, the intensity of the OH and the C—O component peaks A and B, respectively, were increased. The component peak C corresponding to the amide groups is much lower.

Table V Hydrolysis of Acrylamide Grafted Celgard® 2500 Membranes

	Hydrolysis Conditions			Water Flux		
Experiment No.	Concn	Temp. (°C)	Time (min)	Wet (L/m^2 h)	Dry (L/m^2 h)	Wettability after Drying
10	1*N*	60	15	6.75	6.55	Excellent/translucent
11	1*N*	60	15	9.18	12.8	Excellent/translucent
13	1*N*	60	15	74.00	Nil	Partial/opaque
14	1*N*	60	15	32.00	Nil	Partial/opaque
15	1*N*	60	15	56.00	Nil	Partial/opaque
16	1*N*	60	15	87.00	Nil	Partial/opaque
17	1*N*	60	15	90.00	Nil	Partial/opaque

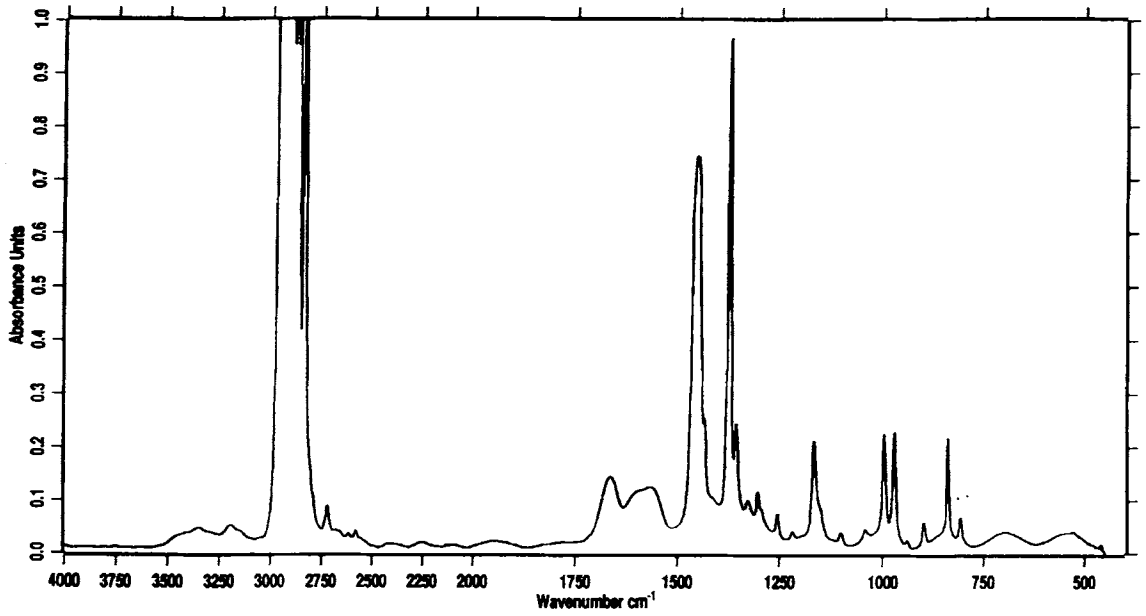

Figure 10 FTIR spectrum (transmission mode) of partially hydrolyzed acrylamide-grafted polypropylene membrane, Celgard® 2500.

The N(1*s*) spectrum [Fig. 11(c)] is divided into two peaks. Peak B (399.70 eV) can be considered for the amide functional groups because it appears at the same position of the N(1*s*) spectrum of hydroxylated and amide-grafted membranes. Furthermore, peak A (400.56 eV) shows the presence of protonated nitrogen on the surface of the hydrolyzed acrylamide-grafted membrane. The component peak for protonated nitrogen species is relatively higher than in the nonhydrolyzed acrylamide-grafted membrane. Obviously, the Brønsted acid carboxyl groups formed by the hydrolysis are able to donate H^+ ions to the basic nitrogen containing groups. In the case of the hydrolyzed membrane, deprotonated carboxyl (COO^-) groups were observed in the FTIR spectrum (absorption band at 1559 cm^{-1}). For the

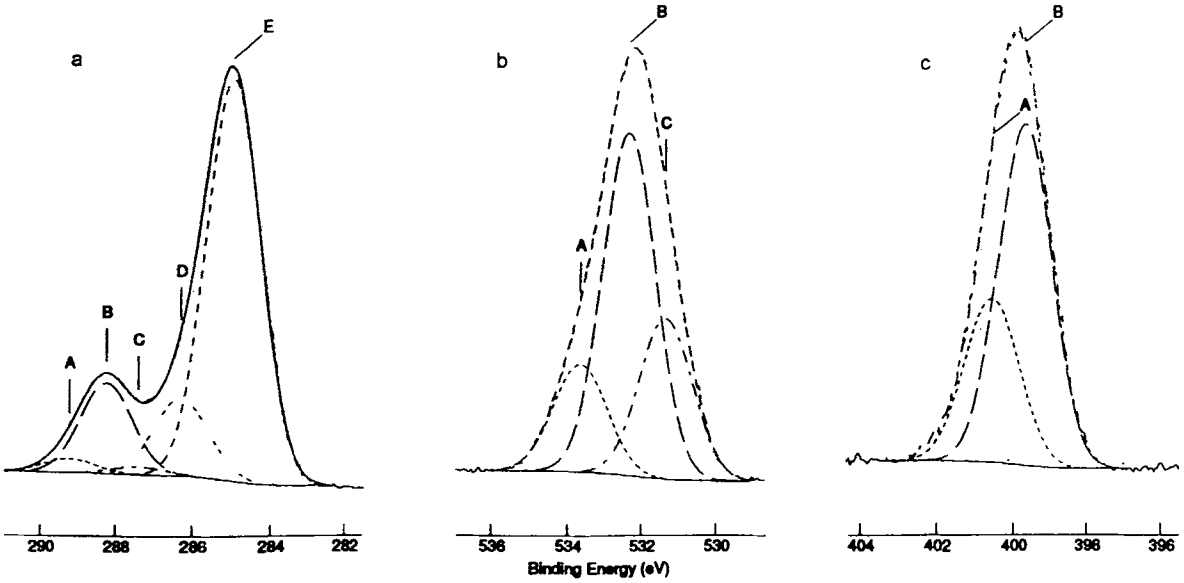

Figure 11 High resolution ESCA spectra (satellites substracted) for partially hydrolyzed acrylamide-grafted polypropylene membrane, Celgard® 2500: (a) C(1*s*) spectrum, (b) O(1*s*) spectrum, and (c) N(1*s*) spectrum.

amide functional groups, the positive charge formed on the nitrogen atom has an influence on the electron density of the oxygen atom adjacent. The oxygen atom gets a positive partial charge and the O(1*s*) peak of this oxygen species shifts to higher binding energies. So the component peak B in the O(1*s*) spectrum presents the protonated amide groups too.

CONCLUSIONS

The microporous PP Celgard® 2400 and 2500 membranes were modified by grafting acrylamide onto the surface to impart hydrophilic properties. The acrylamide-grafted membranes were further partially hydrolyzed to enhance the hydrophilic properties by introducing carboxyl functional groups. This was verified by water contact angle measurements. Before grafting acrylamide, the inert, hydrophobic PP membranes were subjected to oxidative treatment with an aqueous solution of potassium peroxydisulfate to introduce hydroxyl groups onto the membrane surfaces.

It was observed that the hydroxyl groups get buried in the depth of the polymer upon drying, which may be due to the configurational movement of the polymer chains. Therefore, it was essential to preserve the membranes in wet conditions. The acrylamide-grafted and hydrolyzed membranes appeared translucent when immersed in water and allowed water flow even after drying. This indicates that the grafting of acrylamide also takes place within the pores of the membrane. The grafting of acrylamide onto the surface of the interior pore space of PP membranes could be confirmed by FTIR and ESCA analysis. The introduction of amide groups onto the surface of the PP membrane during oxidation with potassium peroxydisulfate under the flow of nitrogen could be confirmed with the ESCA analysis.

The authors are thankful to Dr. A. Schneller of Hoechst AG, Frankfurt/Main for the supply of Celgard® membranes. One of the authors (D.H.G.) gratefully acknowledges the financial assistance given to him in the form of a Guest Scientist fellowship by the Institute of Polymer Research, Dresden, Germany, and is also thankful to the management of GSFC, India, for granting him the study leave.

REFERENCES

1. H. Iwata, A. Kishida, M. Suzuki, Y. Hata, and Y. Ikado, *J. Polym. Sci., Polym. Chem. Ed.*, **26,** 3303 (1984).
2. M. Karakelle and R. J. Zdrahala, *J. Membr. Sci.*, **41,** 305 (1989).
3. Y. J. Wang, C. H. Chen, M. L. Yeh, G. H. Hsiue, and B. C. Yu, *J. Membr. Sci.*, **53,** 275 (1990).
4. A. S. Hoffman, *J. Appl. Polym. Sci., Appl. Polym. Symp.*, **46,** 341 (1990).
5. C. C. Wang and G. H. Hsiue, *J. Appl. Polym. Sci.*, **50,** 1141 (1993).
6. M. Kim, K. Saito, and F. Furusaki, *J. Membr. Sci.*, **56,** 289 (1992).
7. J. Neel, *Makromol. Chem., Macromol. Symp.*, **70/71,** 327 (1993).
8. T. Hirotsu, in *Pervaporation Membrane Separation Processes*, R. Y. M. Huang, Ed., Elsevier Science Publishers B. V., Amsterdam, 1991, p. 461.
9. B. Gupta and G. G. Scherer, *Chimia*, **48,** 127 (1994).
10. I. Ishigaki, T. Sogo, K. Senoo, T. Takayama, S. Machi, J. Okamoto, and T. Okada, *Rad. Phys. Chem.*, **18,** 899 (1981).
11. M. Wada, *Polym. Adv. Technol.*, **5,** 645 (1994).
12. I. Ishigaki, T. Sugo, T. Takayama, T. Okada, J. Okamoto, and K. Senoo, *J. Appl. Polym. Sci.*, **27,** 1043 (1982).
13. N. R. Lazer, U.S. Pat. 4,346,142 (1982).
14. K. Kushi, I. Sasaki, and T. Hiroshi, Jpn. Pat. Sho 61[1986]-86908 (1986).
15. K. J. Kim, A. G. Fane, and C. J. D. Fell, *J. Membr. Sci.*, **46,** 187 (1989).
16. H. Taskier, U.S. Pat. 3,929,509 (1975).
17. H.-M. Buchhammer, G. Petzold, and K. Lunkwitz, Eur. Pat. 0603 987 A1 (1993).
18. M. Nyström, Proc. 1990, Int. Congr. Membr. Membr. Processes (ICOM'90), 1990, p. 90.
19. M. Nyström and P. Järvinen, *J. Membr. Sci.*, **60,** 275 (1991).
20. E. M. Gabriel and G. E. Gillberg, *J. Appl. Polym. Sci.*, **48,** 2081 (1993).
21. K. Yamada, *J. Appl. Polym. Sci.*, **44,** 993 (1992).
22. Z. P. Yao and B. Ranby, *J. Appl. Polym. Sci.*, **40,** 1647 (1990).
23. J. A. Lanuze and D. L. Myers, *J. Appl. Polym. Sci.*, **40,** 595 (1990).
24. M. Strobel, C. Dunatov, J. M. Strobel, C. S. Lyons, S. J. Perron, and M. C. Morgan, *J. Adhesion Sci. Technol.*, **3,** 321 (1989).
25. D. Briggs, D. M. Brewis, and M. B. Konieczko, *J. Mater. Sci.*, **14,** 1344 (1979).
26. I. Sutherland, D. M. Brewis, R. J. Heath, and E. Sheng, *Surface Interface Anal.*, **17,** 507 (1991).
27. D. Briggs, D. M. Brewis, and M. B. Konieczo, *J. Mater. Sci.*, **11,** 1270 (1976).
28. H. A. Willis and V. J. I. Zichy, in *Polymer Surfaces*, D. T. Clark and W. J. Feast, Eds., Wiley, New York, 1978, Chap. 15.
29. J. Peeling and D. T. Clark, *J. Polym. Sci., Polym. Chem. Ed.*, **21,** 2047 (1983).
30. J. Yamauchi, A. Yamaoka, K. Ikemoto, and T. Matsui, *J. Appl. Polym. Sci.*, **43,** 1197 (1991).

31. D. E. Bergbreiter, *Prog. Polym. Sci.*, **19,** 529 (1994).
32. H. Yasuda, *Makromol. Chem., Macromol. Symp.*, **70/71,** 29 (1993).
33. D. L. Cho and Ö. Eckengren, *J. Appl. Polym. Sci.*, **47,** 2125 (1993).
34. T. Hirotsu and A. Arita, *J. Appl. Polym. Sci.*, **42,** 3255 (1991).
35. I. K. Mehta, S. Kumar, G. H. Chauhan, and B. N. Mishra, *J. Appl. Polym. Sci.*, **41,** 1171 (1993).
36. K. Saito, T. Yamaguchi, K. Uezu, S. Furusaki, T. Sugo, and J. Okamoto, *J. Appl. Polym. Sci.*, **39,** 2153 (1990).
37. N. Kabay, A. Katakai, T. Sugo, and H. Egawa, *J. Appl. Polym. Sci.*, **49,** 599 (1993).
38. J. Okamoto, *Radiat. Phys. Chem.*, **29,** 469 (1987).
39. C. H. Bamford and K. G. Al-Lamee, *Macromol. Rap. Commun.*, **15,** 379 (1994).
40. *Celgard Membrane Information Brouchure,* Hoechst Celanese Corporation, USA, 1988.
41. C. D. Wagner, L. E. Davis, M. V. Zeller, J. A. Tayler, R. M. Raymond, and L. H. Gale, *Surface Interface Anal.*, **3,** 211 (1981).
42. C. H. Bamford and K. G. Al-Lamee, *Polymer,* **35,** 2844 (1994).
43. R. P. Singh, *Prog. Polym. Sci.*, **17,** 251 (1992).
44. F. Poncin-Epaillard, B. Chevet, and J. C. Brosse, *J. Appl. Polym. Sci.*, **53,** 1291 (1994).
45. M. B. Huglin, B. L. Johnson, and R. W. Richards, *J. Polym. Sci., Polym. Chem. Ed.*, **14,** 1363 (1976).
46. A. Chapiro and P. Seidler, *Eur. Polym. J.*, **1,** 189 (1965).
47. A. Narebska and Z. Bukowski, *Makromol. Chem.*, **186,** 1425 (1985).
48. J. Friedrich, I. Loeschke, and J. Gähde, *Acta Polym.*, **37,** 687 (1986).
49. D. L. Cho, P. M. Claesson, C. G. Gölander, and K. Johansson, *J. Appl. Polym. Sci.*, **41,** 1373 (1990).
50. H. Yasuda and A. K. Sharma, *J. Polym. Sci., Polym. Phys. Ed.*, **19,** 1285 (1981).
51. E. M. Cross and T. J. McCarthy, *Macromolecules,* **23,** 3916 (1990).
52. R. R. Holmes-Farley and R. H. Reamey, *Langmuir,* **3,** 799 (1987).
53. N. Watanabe, Y. Ashida, and T. Nakajima, *Bull. Chem. Soc., Jpn.*, **55,** 3197 (1982).
54. Y. Taru and K. Takaoka, *Kobunshi Ronbunshu,* **43,** 361 (1986).
55. A. Garton, *Infrared Spectroscopy of Polymer Blends, Composites and Surfaces,* Hanser Publishers, Munich, 1992.
56. G. Beanson and D. Briggs, in *High Resolution XPS of Organic Polymers,* Wiley, New York, 1992.

Received March 3, 1995
Accepted November 22, 1995